ULTRAFINE-GRAINED MATERIALS

Evolution of microstructure of an iron aluminide during severe plastic deformation by heavy rolling

**D. G. Morris · I. Gutierrez-Urrutia ·
M. A. Muñoz-Morris**

Abstract Severe plastic deformation is generally achieved using novel techniques such as Equal Channel Angular Pressing (ECAP) or High Pressure Torsion (HPT), but may also be achieved by more conventional methods such as very heavy rolling. Microstructure evolution is examined in an iron aluminide intermetallic rolled to strains up to 3.3 using Transmission Electron Microscopy (TEM) and orientation determinations by Kikuchi line analysis. After the highest strains the microstructure is still characterized as a recovered submicron-scale dislocation structure, with generally low angles across the various boundaries, and a high density of dislocations inside these boundaries. The structures observed show a dependence on orientation of the underlying parent grain, with [001] orientations showing poorer rearrangement to cellular structures than grains with [113–111] orientations.

Introduction

Severe plastic deformation is an important method to obtain refined microstructures in ductile alloys, of scale varying from the micron to the significantly sub-micron level, depending on the amount of recovery during deformation. Hansen et al. [1] described the organization, from low strain levels, of dislocations produced by deformation into a cell block structure with internal dislocation cell boundaries. These cell blocks, separated by dense dislocation walls (DDW) or Microbands (MB) are considered to be produced by the accumulation of geometrically necessary dislocations (GND). Cell boundaries form inside these cell blocks, presumably by the accumulation of incidental dislocations, and may be called incidental dislocation boundaries (IDB). Misorientations between the cell blocks tend to be large and, as additional dislocations consolidate these walls, they gradually change to high angle grain boundaries (HAGB), in contrast to cell boundaries (or IDB) which maintain only small misorientations. With increased straining, the cell blocks become finer, with elongated morphology along the straining (e.g rolling) direction, and eventually lose the internal cell boundaries as the cell block size refines to near the cell size. Such microstructures have been reported for various deformed fcc materials [1, 2], and a crystal orientation dependence of deformation structures also noted. Thus, grains with [001] orientations tend to retain cell structures, whilst grains with [111–112–113] orientations show a stronger accumulation of the DDW/MB, cell block structure. An orientation dependence of microstructure has also been noted during deformation by rolling of ferritic alloys, where cube-oriented grains are seen to be more stable against building up large orientation gradients [3], which are important to allow easy recrystallization during subsequent annealing [4, 5].

Plastic deformation to higher strain levels is achieved by processes such as Equal Channel Angular Pressing (ECAP) or High Pressure Torsion (HPT), but only rarely has microstructure been fully characterized. Valiev et al. [6] examined Fe deformed to strains of about 300 by HPT and characterized the microstructure as a dislocation cell structure, gradually changing to a nanograin structure at the highest strains. Zhilyaev et al. [7] observed equiaxed nanograins separated by random HAGB after straining Ni to similarly high strains. The intermediate strain levels (5–6) typically produced by ECAP tend to produce an

D. G. Morris (✉) · I. Gutierrez-Urrutia · M. A. Muñoz-Morris
Department of Physical Metallurgy, CENIM, CSIC, Avenida
Gregorio del Amo 8, 28040 Madrid, Spain
e-mail: david.morris@cenim.csic.es

elongated dislocation cell structure in bcc steels, where average boundary misorientations are relatively low [8]. Similar results have been reported for ferritic and duplex steels deformed to high strains using various methods [9, 10], with average boundary misorientations gradually increasing with strain. The orientation sensitivity of microstructure mentioned above has been reported during severe plastic deformation, e.g. in Ni_3Al deformed by HPT [11, 12]. A dislocation subgrain structure gradually transformed to a nanocrystalline structure at strains of 100–400, with the nanostructure appearing for grains oriented near [112] whilst recovered microcrystalline structures remained for grains oriented near [001].

The present study examines changes of microstructure in an ordered bcc intermetallic, based on Fe_3Al, as deformation increases up to high strain levels during conventional rolling. Of especial interest is to analyse the type of microstructure obtained—dislocation density, boundary spacings and misorientations—and to relate this to the imposed strain level. Such information is of great relevance when attempting to interpret strengthening, as will be reported elsewhere.

Experimental details

The material studied was a Fe_3Al-base alloy of composition Fe–27.8%Al-5.0%Cr-0.1%Zr (atomic percent), initially in the form of warm rolled strip of thickness 1 mm. It was given a prior anneal to produce an equiaxed grain size of about 100 μm. Rolling was carried out at room temperature using a laboratory rolling mill with 8 cm diameter rolls rotating at approximately one turn per second. Rolling was carried out applying several passes with approximately 10% reduction per pass, with samples taken at strain levels of 0.4 (33% reduction), 1.4 (75% reduction), 2.3 (90% reduction) and 3.3 (96–97% reduction). Edge cracking of the strip was noticed after about 40% reduction, increasing in importance with strain, such that by 90–96% reduction the cracks essentially crossed the entire strip, leaving samples of about 1 cm in size. Material was examined in the as-rolled state, and also after an annealing treatment of 1 h at 600 °C, which leads to significant recovery of microstructure with little or no recrystallization.

Microstructures were examined on electropolished thin foils by both Scanning Electron Microscopy (SEM) and Transmission Electron Microscopy (TEM). SEM, with back-scattered electron contrast, was used to confirm microstructural homogeneity and to detect recrystallization in annealed materials. Determination of boundary misorientations by SEM was difficult, in view of the highly strained, fine microstructure present, and hence TEM was used. Both bright field and dark field/weak beam imaging was used for general structure analyses and for determination of dislocation densities. Misorientations across the various boundaries were determined in two ways: an overall impression of large scale orientation changes was obtained by Selected Area Diffraction (SAD) using a large aperture of 2 μm diameter (covering typically 10–40 cellular regions); individual cell orientations were determined from Kikuchi pattern analysis using a low camera constant and converging the electron beam within the single cell—many neighbouring regions were examined to allow the determination of misorientation of about 100 boundaries per state.

Results

Microstructural evolution

The most important aspects of microstructure evolution during straining are illustrated in Fig. 1, with quantitative information given in Table 1. At a very early stage of deformation (strain level 0.4) the microstructure is characterized by a high dislocation density with only a slight tendency to rearrangement as dislocation cells, Fig. 1a. With increasing strain, the dislocations rearrange to a cellular structure whereby the cell walls remain loosely defined, and a high dislocation density is retained within the cell interiors, Fig. 1d–f. Cell morphology is somewhat elongated along the rolling direction, marked by an arrow in each case in Fig. 1, and cell size refines continuously over the strain range examined, see Table 1. For grain orientations close to [001] the cellular arrangement appears slightly less marked than for other orientations, [113–111], compare Fig. 1b with Fig. 1c, and Fig. 1d with Fig. 1e. The first pair (Fig. 1b, c) compares structures in deformed and recovered samples, whilst the second pair (Fig. 1d, e) compares structures in the as-deformed states. Annealing for 1 h at 600 °C leads to a major decrease in the loose dislocation density within the cells and the dislocations constituting the cell boundaries rearrange to a sub-boundary structure, see Fig. 1b and c. Note that grains with [113–111] orientation show a stronger cellular/subgrain arrangement than do grains with [001] orientation, compare Fig. 1b with Fig. 1c, retaining the orientation sensitivity of the deformed state. These observations make it clear that the microstructure obtained is a typical deformation structure of loose dislocations and dislocation cells, and should not be described as a sub-micron grain structure, even for the relatively high final strain examined (3.3).

Boundary misorientations

Some examples of the determination of cell orientations and of boundary misorientations are given in Fig. 2. Examination of a relatively large area (circle of about 2 μm diameter) by SAD shows a spread of the diffraction spots, typically

Fig. 1 Microstructures after deformation by rolling, some annealed: (**a**) deformed 0.4; (**b**) deformed 1.4, annealed 600 °C, orientation near [001]; (**c**) deformed 1.4, annealed 600 °C, orientation near [113]; (**d**) deformed 2.3, orientation near [001]; (**e**) deformed 2.3, orientation near [111]; and (**f**) deformed 3.3, orientation near [111]. Rolling direction is marked in each case
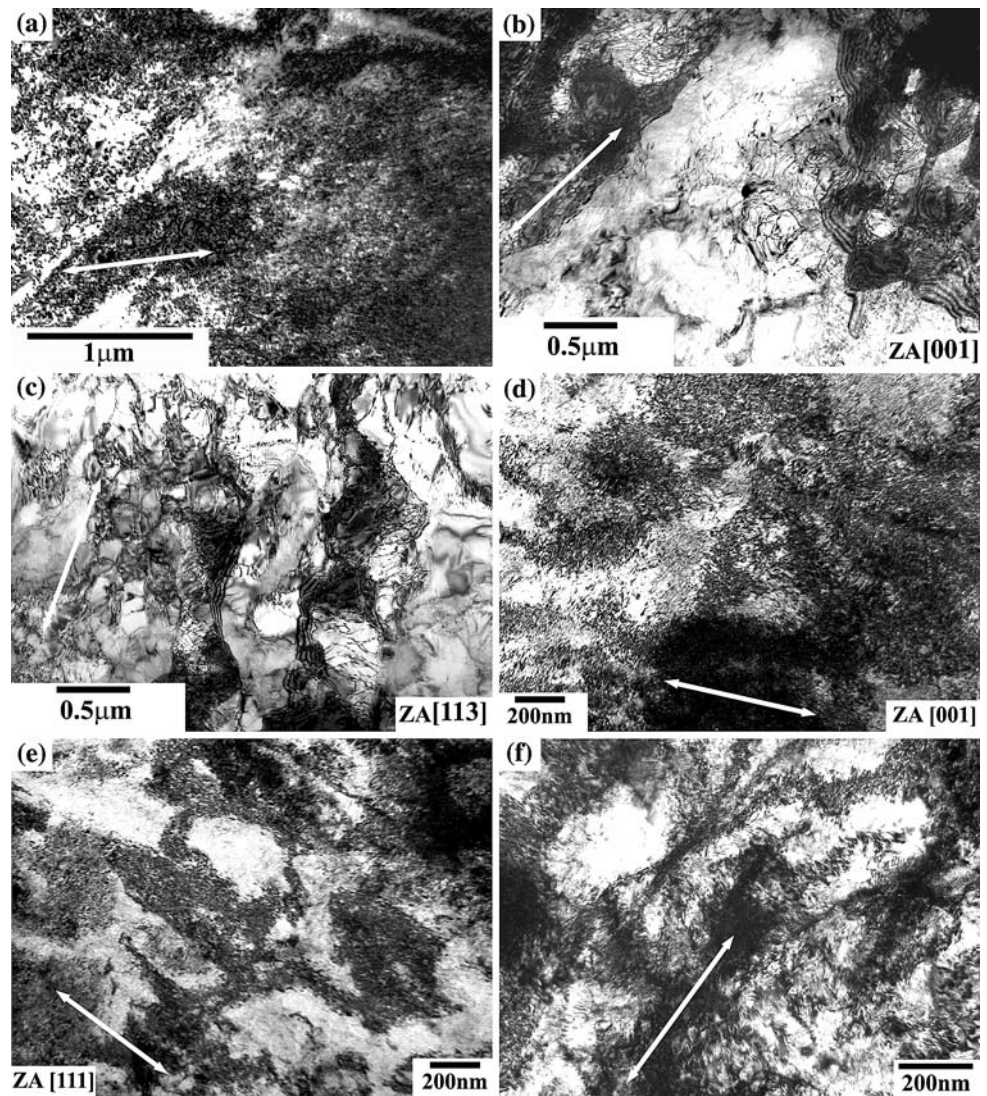
over some 5–10° corresponding to the changes of orientation of the 10–40 cellular regions examined. This misorientation spread is shown in Table 1 as the parameter $\Delta\theta$, and is seen to increase steadily with strain, from a few degrees to about 10° after the highest strain examined. Figure 2 shows also the identification of precise cell orientation by Kikuchi line analysis on three neighbouring cells—for material with grain orientation close to [113]. The cell boundary separating neighbouring cells 1 and 2 is about 12°, whereas the boundary separating neighbouring cells 2 and 3 is about 2°. This variation of misorientation from some boundaries to others seems to correspond to the low-angle cell walls (IDB) and cell block walls (DDW) characteristic of deformation structures. Figure 3 gives one example of analysis of boundary misorientations in another deformed-annealed material, showing that many boundaries are of very low angles (1–5°), with some regions showing much higher boundary misorientations (8–14°).

Misorientations were determined using such Kikuchi line analysis for all the deformed and the annealed materials, and some examples are shown in Fig. 4. The ranges of individual boundary misorientations observed ($\delta\theta$), as well as the average values, are given in Table 1. Figure 4 shows that most boundaries have very low misorientations, only a few degrees, for strains to 2.3, and it is only after the highest strain of 3.3 that significant numbers of medium-angle boundaries (approximately 8–15°) appear. Taking the usual definition of 15° misorientation to characterize a normal (high angle) grain boundary, it is clear that strains above 3.3 are required for grain size to be significantly refined. The information given in Table 1 confirms this gradual increase in boundary misorientation. Figure 4 and Table 1 also confirm that the orientation sensitivity of dislocation rearrangement into the cellular structures is not reflected in the misorientations produced. Thus, boundaries formed by deformation in grains with [001] orientations

Table 1 Summary of microstructural analyses

Strain level	33% (true 0.4)	75% (true 1.4)		90% (true 2.3)		96% (true 3.3)	
As deformed							
Grain orientation		[111]	[001]	[111]	[001]	[111]	[001]
Cell size (nm)	∼500	330	400	250	300	190	∼400
$\Delta\theta$ (°)	0.5–1	8	7	10 ± 2	8 ± 2	10–20	11–13
$\delta\theta$ range (°)		0.2–13	0.2–11	0.5–17	0.5–15	2–21	
Average $\delta\theta$ (°)	1	4	3.5	6		9.5	
Hardness (Hv, GPa)	3.50	4.03		5.23		5.55	
Annealed 1 h 600 °C							
Microstructural state	Recovery only	Recovery only		Partially recrystallized		Partially recrystallized	
Grain orientation		[111]-[113]	[001]	[111]		[111]	
Cell size (nm)	∼500	330	400–500	240		300	
$\Delta\theta$ (°)	0.5–1	9	7	7–10		10 ± 2	
$\delta\theta$ range (°)		0.4–14	0.3–14	0.5–17		1–19	
Average $\delta\theta$ (°)	1	4	3.5	6		9	
Hardness (Hv, GPa)	3.00	3.35		4.10		4.40	
Recrystallized region	Recrystallization began at ∼500 h; grain size 17 μm	Recrystallization began at ∼10 h; grain size 6–7 μm		22%; grain size 4 μm		20%; grain size 5 μm	

$\Delta\theta$ is orientation spread found in large aperture SAD patterns; $\delta\theta$ is misorientation measured across boundaries using Kikuchi patterns

Fig. 2 Examples of determination of overall lattice rotations by SAD (**a**) and of precise orientation of individual cell regions by Kikichi line analysis (**b–d**): material deformed 1.4 and annealed at 600 °C
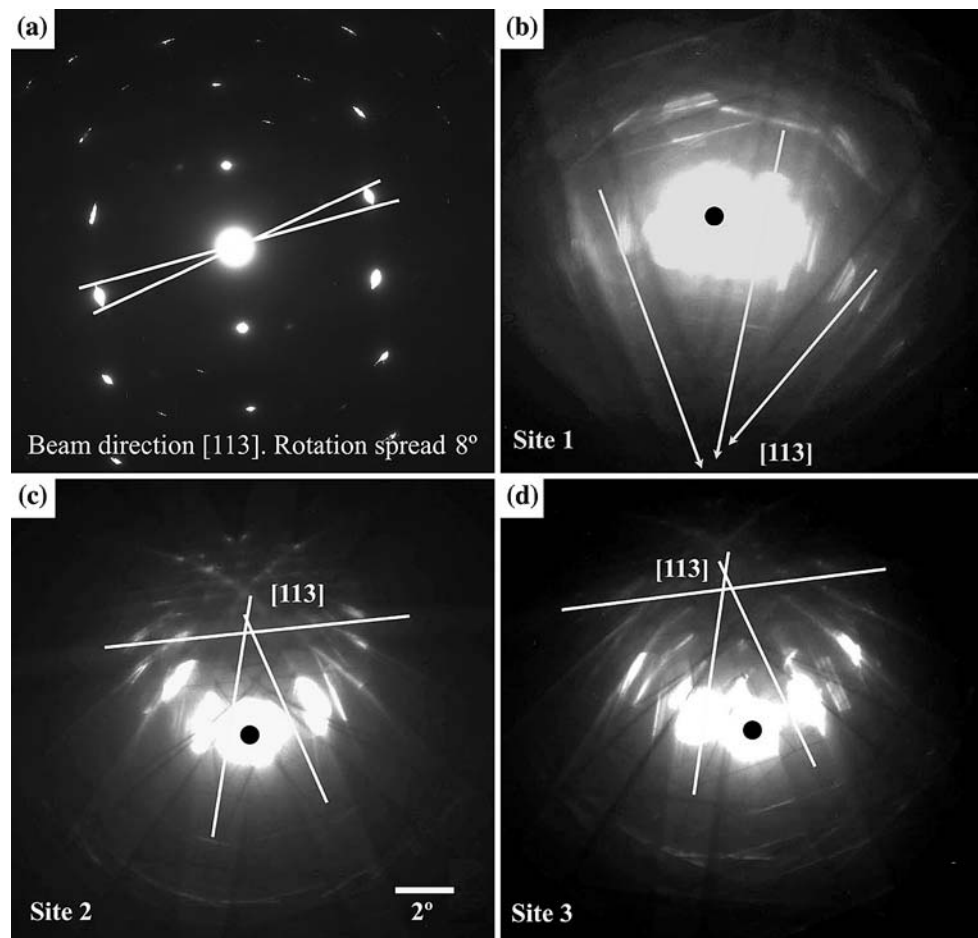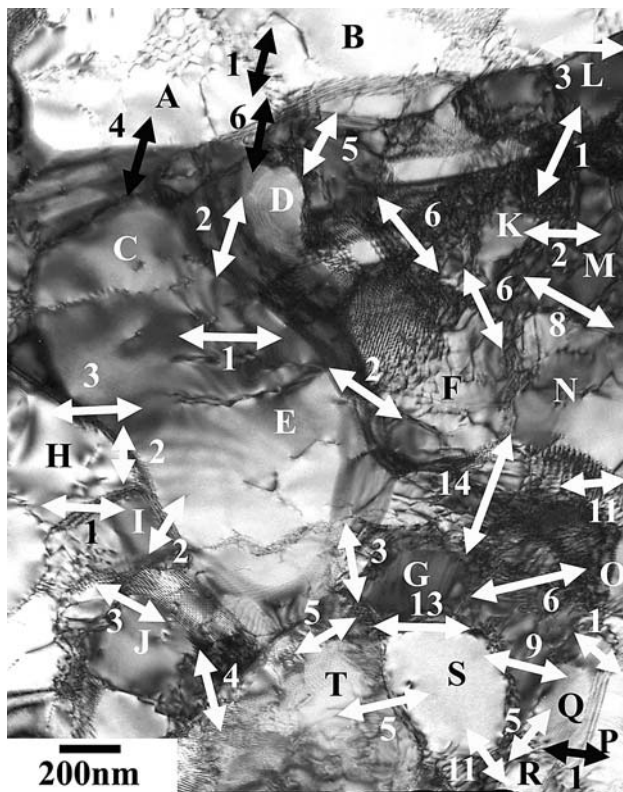
Fig. 3 Analysis of cellular areas and misorientations between them. Material deformed 2.3 and annealed at 600 °C

show a similar range of misorientations to those formed in grains with [113–111] orientations. The orientation sensitivity of cellular arrangement seen in the micrographs, Fig. 1, is produced by a different extent of dislocation recovery even though the initial dislocation density or associated lattice rotation is the same.

Material hardness

Microhardness values of as-deformed and subsequently annealed samples are given in Table 1, and show a steady increase with strain. Annealing for recovery (1 h at 600 °C) produces a relatively small hardness decrease. It is beyond the scope of the present short paper to analyse the origin of this hardening and softening, but it is clear that the hardening cannot be ascribed to grain size refinement, since only few HAGB are produced. Detailed analysis, to be reported elsewhere, shows that both loose dislocation hardening and cell-wall hardening contribute to the hardness increase.

Effect of annealing on microstructural recovery

The heat treatment of 1 h at 600 °C reported here led only to recovery for materials deformed to 0.4–1.4. Continued
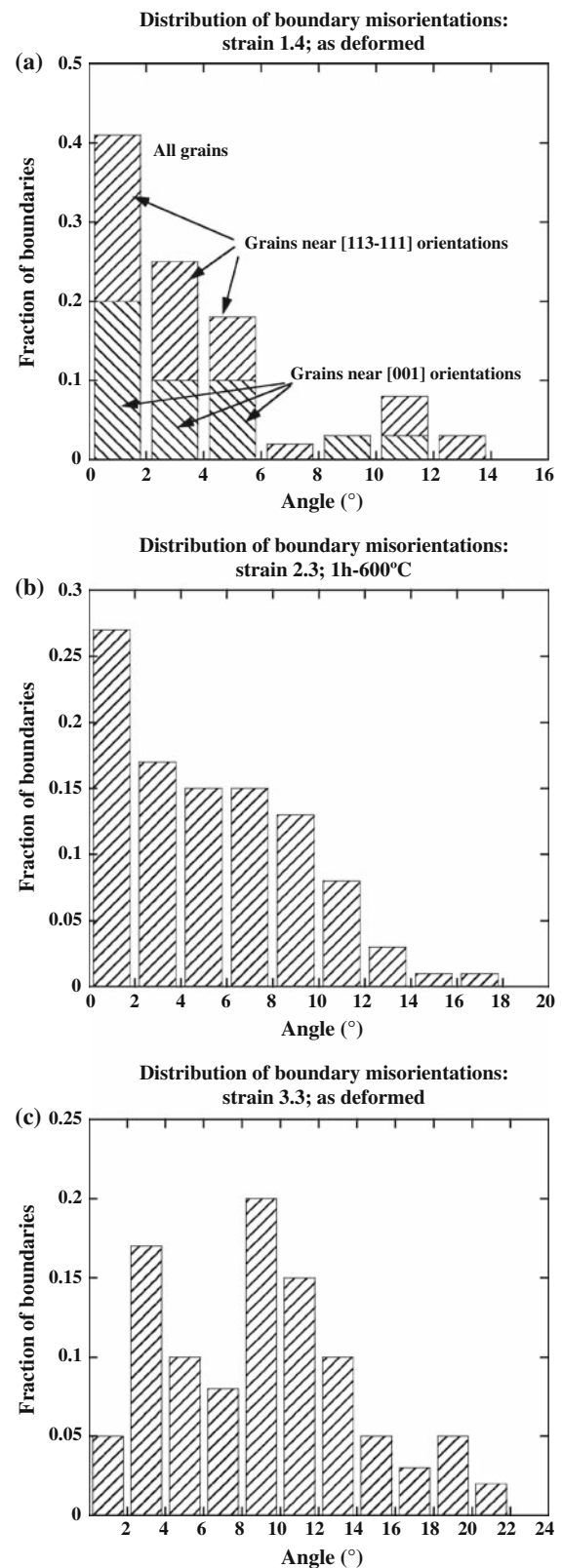
Fig. 4 Histograms showing distribution of boundary misorientations for materials: (**a**) deformed 1.4; (**b**) deformed 2.3 and annealed at 600 °C; and (**c**) deformed 3.3

heat treatments [13] led to eventual fuller recovery and recrystallization, with large final grain sizes, see Table 1. The heavily deformed materials showed incipient recrystallization after 1 h at 600 °C, and further annealing led to recrystallization with fine grain sizes (several microns), Table 1. Clearly the driving force for recrystallization, as well as the availability of suitable nuclei for new grain formation, depends strongly on the density of dislocations and cell walls as well as the presence of relatively high angle boundaries formed already during the deformation.

Discussion and summary

The present study emphasizes that strains significantly above 3–4 are required to produce a (sub-micron) grain structure as opposed to the high dislocation density with cell structure found at lower strains. This is reflected in the very gradual increase in average boundary misorientation and the fraction of HAGB. The absence of recovery and recrystallization during deformation means that the material is characterized by a high dislocation density and low-angle dislocation walls. Simultaneous or subsequent recovery and recrystallization is required to obtain a boundary-controlled material, submicrocrystalline or nanocrystalline.

No role of order has been discussed here for the simple reason that order is lost from the early stages of deformation [13], reappearing only during subsequent annealing.

While special techniques such as ECAP or HPT are required to achieve extremely high strains, methods such as the conventional rolling used here are able to provide sufficient strains for many of the microstructures and property advantages of severe plastic deformation to be demonstrated.

At the same time the importance of analysing all the boundaries present, especially the significant number of very low angle boundaries always present, is emphasized. This is a significant reason to justify the use of TEM for analysis. The low-angle boundaries represent a significant fraction of the total boundaries present up to high strains and contribute significantly to hardening.

The present work contributes to our understanding of how structure evolves during straining, as summarized in Fig. 5. This figure covers the full range of strains that have been explored experimentally using typical forming methods (e.g. rolling) for small strains (0.1–3) [1, 2, 9], ECAP for higher strains (2–10) [8, 10], HPT for much larger strains (10–300) [6, 7, 11, 12] and mechanical milling (MM) for even greater strains (>300) [14, 15]. While the microstructure scale, indicated by the closed points, decreases continuously with increased strain, it is over the strain range approximately 3–10 where a predominantly cell structure is converted to a predominantly
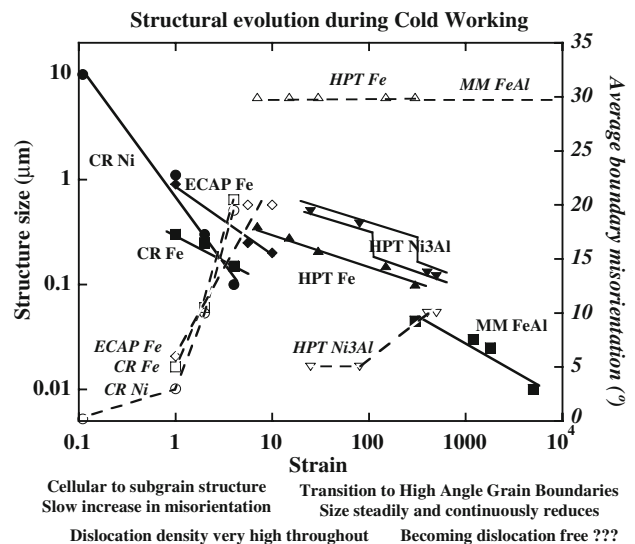
Fig. 5 Diagram showing structural evolution (boundary spacing, and misorientation across boundaries) with increasing strain. Data taken from references [1, 2, 6–12, 14, 15]. Closed points indicate microstructure size (i.e. cell or grain size), whilst open points indicate average boundary misorientation. Processing method and material are indicated in each case (CR = cold rolling; ECAP, HPT and MM have been defined in the text). Two data lines are shown for HPT refinement of grain size of Ni$_3$Al [11, 12], referring to an orientation dependence of refinement, see text for details

grain structure, as indicated by the open points showing boundary misorientations. The orientation of the original grain is seen to play a role, presumably through the selection of deformation systems [1, 2], in the dislocation structures produced and their recovery into cellular structures, as well as their conversion into nanocrystalline grain regions at higher strains [11, 12]. As seen in the present work, crystal orientations close to [001] recover to a cellular structure more slowly than orientations near [113]-[111]. The previous study on Ni$_3$Al [11, 12] showed slower transformation to nanostructures for orientations near [001] than for those near [113]-[111], as indicated by the two lines for grain refinement in Ni$_3$Al shown in Fig. 5.

References

1. Hansen N, Huang X, Highes DA (2001) Mater Sci Eng A 317:3. doi:10.1016/S0921–5093(01)01191-1
2. Mishin OV, Juul Jensen D, Hansen N (2003) Mater Sci Eng A 342:320. doi:10.1016/S0921-5093(02)00311-8
3. Raabe D, Zhao Z, Park SJ, Roters F (2002) Acta Mater 50:421. doi:10.1016/S1359-6454(01)00323-8
4. Raabe D, Mao W (1995) Philos Mag A 71:805. doi:10.1080/01418619508236221

5. Kobayashi S, Zaefferer S, Schneider A, Raabe D, Frommeyer G (2004) Mater Sci Eng A 387–389:950. doi:10.1016/j.msea.2004.02.086

6. Valiev RZ, Ivanisenko Yu V, Rauch EF, Baudelet B (1996) Acta Mater 44:4705. doi:10.1016/S1359-6454(96)00156-5

7. Zhilyaev AP, Nurislamova GV, Kim B-V, Baró MD, Szpunar JA, Langdon TG (2003) Acta Mater 51:753. doi:10.1016/S1359-6454(02)00466-4

8. Lin H, Xu C, Han BQ, Lavernia EJ, Langdon TG (2004) In: Zhu YT, Langdon TG, Valiev RZ, Semiatin SL, Shin DH, Lowe TC (eds) Ultrafine grained materials III. TMS (The Minerals, Metals and Materials Society), USA, p 523

9. Belyakov A, Kimura Y, Tsuzaki K (2006) Acta Mater 54:2521. doi:10.1016/j.actamat.2006.01.035

10. Todaka Y, Umemoto M, Yin J, Liu Z, Tsuchiya K (2007) Mater Sci Eng A 462:264. doi:10.1016/j.msea.2006.03.150

11. Rentenberger C, Karnthaler HP (2005) Acta Mater 53:3031. doi:10.1016/j.actamat.2005.03.016

12. Rentenberger C, Karnthaler HP (2007) Int J Mater Res 98:255

13. Morris DG, Gunther S (1995) Intermetallics 3:483. doi:10.1016/0966-9795(95)00007-L

14. Morris-Muñoz MA, Dodge A, Morris DG (1999) Nanostructured Mater 11:873. doi:10.1016/S0965-9773(99)00385-2

15. Courtney TH, Aikin BJM, Maurice D, Rydin RW, Kosmac T (1993) In: deBarbadillo JJ, Froes FH, Schwarz R (eds) Mechanical alloying for structural applications. ASM, Materials Park, p 1